

Article

From Sun to Interplanetary Space: What is the Pathlength of Solar Energetic Particles?

Laitinen, Timo Lauri mikael and Dalla, Silvia

Available at <https://clock.uclan.ac.uk/31346/>

Laitinen, Timo Lauri mikael orcid iconORCID: 0000-0002-7719-7783 and Dalla, Silvia orcid iconORCID: 0000-0002-7837-5780 (2019) From Sun to Interplanetary Space: What is the Pathlength of Solar Energetic Particles? The Astrophysical Journal, 887 (2). p. 222. ISSN 0004-637X

It is advisable to refer to the publisher's version if you intend to cite from the work.
<http://dx.doi.org/10.3847/1538-4357/ab54c7>

For more information about UCLan's research in this area go to
<http://www.uclan.ac.uk/researchgroups/> and search for <name of research Group>.

For information about Research generally at UCLan please go to
<http://www.uclan.ac.uk/research/>

All outputs in CLoK are protected by Intellectual Property Rights law, including Copyright law. Copyright, IPR and Moral Rights for the works on this site are retained by the individual authors and/or other copyright owners. Terms and conditions for use of this material are defined in the [policies](#) page.



From Sun to Interplanetary Space: What is the Pathlength of Solar Energetic Particles?

T. Laitinen and S. Dalla

Jeremiah Horrocks Institute, University of Central Lancashire, Preston, UK; tlmlaitinen@uclan.ac.uk

Received 2019 July 12; revised 2019 October 9; accepted 2019 November 4; published 2019 December 20

Abstract

Solar energetic particles (SEPs), accelerated during solar eruptions, propagate in turbulent solar wind before being observed with in situ instruments. In order to interpret their origin through comparison with remote sensing observations of the solar eruption, we thus must deconvolve the transport effects due to the turbulent magnetic fields from the SEP observations. Recent research suggests that the SEP propagation is guided by the turbulent meandering of the magnetic fieldlines across the mean magnetic field. However, the lengthening of the distance the SEPs travel, due to the fieldline meandering, has so far not been included in SEP event analysis. This omission can cause significant errors in estimation of the release times of SEPs at the Sun. We investigate the distance traveled by the SEPs by considering them to propagate along fieldlines that meander around closed magnetic islands that are inherent in turbulent plasma. We introduce a fieldline random walk model which takes into account the physical scales associated to the magnetic islands. Our method remedies the problem of the diffusion equation resulting in unrealistically short pathlengths, and the fractal dependence of the pathlength of random walk on the length of the random-walk step. We find that the pathlength from the Sun to 1 au can be below the nominal Parker spiral length for SEP events taking place at solar longitudes 45E to 60W, whereas the western and behind-the-limb particles can experience pathlengths longer than 2 au due to fieldline meandering.

Unified Astronomy Thesaurus concepts: [Solar energetic particles \(1491\)](#); [Heliosphere \(711\)](#); [Interplanetary turbulence \(830\)](#); [Interplanetary physics \(827\)](#)

1. Introduction

A central goal of modeling solar energetic particle (SEP) propagation in the heliosphere is to uncover the relative timing between the SEP production at the Sun and the remote-sensed multiwavelength observations of the solar eruption responsible for the SEP event. As the interplanetary medium is permeated with a magnetic field which on average has a Parker spiral shape (Parker 1958), overlaid with turbulence, the charged SEP transport is stochastic in nature. The physics of the turbulence evolution, the SEP transport parameters, and indeed the behavior of the charged particles in such turbulent magnetic fields are not fully understood.

As the SEP transport is controlled by stochastic processes, it is often modeled by use of a diffusion description, typically via a Parker or Fokker–Planck transport equation with diffusion terms to describe the stochasticity of the propagation (e.g., Parker 1965; Jokipii 1966). Several researchers have used 1D propagation models with pitch angle diffusion to fit SEP data in order to deconvolve the interplanetary transport from SEP observations (see, e.g., Kallenrode 1993; Torsti et al. 1996; Laitinen et al. 2000; Dröge 2003; Agueda et al. 2009; Gómez-Herrero et al. 2015).

Full deconvolution of the interplanetary transport from SEP observations, however, is complicated and usually performed only in case studies. As an alternative, timing analysis of SEPs is often used to connect the SEPs to the solar remote sensing observations, particularly in large statistical studies.

In particular the velocity dispersion analysis (VDA) method is often used to obtain the time of SEP injection near the Sun from the SEP onset times at 1 au (e.g., Lin et al. 1981; Reames et al. 1985; Torsti et al. 1998; Krucker & Lin 2000; Tylka et al. 2003; Dalla et al. 2003; Reames 2009; Vainio et al. 2013; Paassilta et al. 2018; Zhao et al. 2019). In VDA, the first particles are assumed to be injected simultaneously, and

propagating to the observing spacecraft without scattering. Under these assumptions, the injection time at the Sun, t_{Sun} can be obtained from the observed onsets by fitting

$$t_{oj} = t_{\text{Sun}} + s/v_j \quad (1)$$

to the 1 au onset times t_{oj} of the SEPs propagating with velocities v_j . The pathlength s in Equation (1) is often expected to be the local Parker spiral length, around 1.1–1.2 au; however, the statistical studies often show a very large range of pathlengths, from <1 au to over 5 au (e.g., Paassilta et al. 2017). Several modeling studies have addressed the reliability of the VDA method (e.g., Kallenrode & Wibberenz 1990; Lintunen & Vainio 2004; Sáiz et al. 2005; Laitinen et al. 2015; Wang & Qin 2015), showing that the apparent long or short pathlength may be due to the interplanetary scattering conditions and the pre-event background, rather than an indication of the length of the actual traveled pathlength or energy-dependent injection time of SEPs at the Sun, $s_{\text{Sun}}(v_j)$.

Recent observations of SEP events simultaneously with multiple spacecraft offer a different interpretation to long pathlengths. SEP events analyzed by several authors (e.g., Dresing et al. 2012; Wiedenbeck et al. 2013; Cohen et al. 2014; Dröge et al. 2014; Richardson et al. 2014) have demonstrated the ability of SEPs accelerated near the Sun to reach a wide range of heliographic longitudes rapidly. It has been suggested that such a fast spread can be attributed to interplanetary propagation of SEPs across the Parker spiral direction, modeled as cross-field diffusion in several studies (e.g., Zhang et al. 2009; Dröge et al. 2010; He et al. 2011; Dresing et al. 2012). The cross-field diffusion is believed to be dominated by random walk of the magnetic fieldlines, due to turbulent fluctuations, and several theoretical approaches have used this concept to derive spatial cross-field diffusion coefficients (e.g., Jokipii 1966; Matthaeus et al. 2003; Shalchi 2010; Ruffolo

et al. 2012). Recent research points out that the perpendicular propagation of the particles with respect to the mean field at short timescales is not actually diffusive, but systematic propagation along the stochastically meandering fieldlines. These studies (Laitinen et al. 2013, 2016) propose to model the early SEP propagation initially along diffusively meandering fieldlines instead, employing a fieldline diffusion approach (Matthaeus et al. 1995).

The effect of the diffusive perpendicular transport of SEPs on the pathlength was investigated recently by Wang & Qin (2015), using the 3D focused transport equation (e.g., Zhang et al. 2009). They found that particles diffusing across the mean Parker spiral to wide heliolongitudinal separations in general have longer pathlengths than those arriving to well-connected locations at 1 au. Thus, the cross-field propagation of particles gives a possible explanation for the observed long pathlengths of SEPs, as given by the VDA method.

However, as we demonstrate in this study, the approach using spatial diffusion for SEP cross-field propagation has the disadvantage that it may result in unphysically short propagation times and pathlengths. This was recently noted by Strauss & Fichtner (2015), who analyzed SEP transport in the inner heliosphere using a 2D transport equation. They found that in some cases the simulated intensities at 1 au began to rise before an unscattered SEP could have reached that distance, that is, $t_o, j - t_{\text{Sun}} < 1 \text{ au}/v_j$, breaking causality. As discussed by Strauss & Fichtner (2015), and in more detail in our study, this is due to the fact that in diffusion description the effect of diffusive cross-field propagation on propagation time of the particles is not taken into account.

In this paper, we address the problem of determining the pathlength of SEPs in the heliospheric magnetic field by analyzing the length of turbulently meandering magnetic fieldlines, and propose a new method for calculating the pathlength when analyzing SEP events. Our approach is based on the nonlinear formulation of fieldline diffusion, where the diffusion coefficient is proportional to the ultrascale $\tilde{\lambda}$ (Matthaeus et al. 1995) instead of the correlation scale as in the earlier quasilinear approach, e.g., Jokipii & Parker (1968). The ultrascale is identified as the size scale of turbulent magnetic islands (e.g., Matthaeus et al. 1999), thus $\tilde{\lambda}$ provides an ideal scale for derivation of the length of turbulently meandering fieldlines, which control the particle propagation in magnetic turbulence.

Our approach in the present study only accounts for the effect of particles propagating on meandering fieldlines on the pathlength of the particles. For consistent analysis of SEP propagation, our results must be implemented in an SEP transport model that contains parallel scattering and drifting of SEPs from their fieldlines due to both stochastic and large-scale gradients and curvatures such as those cited above. Such a model can provide realistic estimates for SEP events observed in the interplanetary space for a wide range of source and transport conditions.

The paper is organized as follows: In Sections 2.1 and 2.2 we discuss the difficulties in determining the pathlength of a stochastically propagating particle. We introduce a novel method to determine the pathlength in Sections 2.3 and 2.4, based on the scale size of turbulent magnetic islands that guide the random-walk of the meandering fieldlines. In Section 3 we outline simulations of stochastically meandering fieldlines in Parker spiral geometry, and show the resulting pathlengths in

Section 4. We discuss the implications of our work in Section 5 and draw conclusions in Section 6.

2. Pathlength in Cartesian Geometry

2.1. Pathlength and Diffusion Equation

Propagation of SEPs along and across the mean magnetic field is typically modeled using a spatial convection–diffusion description, such as the Fokker–Planck descriptions based on works by several authors (e.g., Parker 1965; Zhang et al. 2009). Here we will first concentrate on a very simple form of such an equation, given for propagation of particles along constant magnetic field, $\mathbf{B} = B_0 \hat{z}$, with constant velocity v , and diffusion across it in the x -direction with a constant diffusion coefficient κ . Under these conditions, the convection–diffusion equation for the particle density $n(x, z, t)$ can be written in a Cartesian 2D form as

$$\frac{\partial n(x, z, t)}{\partial t} + v \frac{\partial n(x, z, t)}{\partial z} = \kappa \frac{\partial^2 n(x, z, t)}{\partial x^2}, \quad (2)$$

In this simple model, pitch angle diffusion, which would give rise to diffusion of the particles along the magnetic field direction, is ignored.

Equation (2) and its analytical solution,

$$n(x, z, t) = \frac{n_0(z - vt)}{2\sqrt{\pi\kappa t}} e^{-x^2/(4\kappa t)}, \quad (3)$$

for an impulsive point-injection $n_0 = \delta(t)\delta(x)\delta(z)$, represent an asymptotically valid solution for a random-walk process across the field with a large number of steps, $N \gg 1$, of particle population that propagates along the field with velocity v , and diffuses across the field in the x -direction. However, this solution is unphysical in that the diffusion across the field is not limited by the particle velocity: at a given $z = vt$ the density is nonzero at all x -values.

This unphysical nature of the solution can perhaps be better demonstrated when viewing the solution with the stochastic differential equation (SDE) approach. Diffusion and diffusion-convection equations can be solved using SDEs (e.g., Zhang 1999; Gardiner 2009; Strauss & Effenberger 2017), by use of statistics derived from pseudoparticles that are propagated as given by SDEs that are equivalent to the diffusion equation. In the case of our simple model given by Equation (2), the corresponding SDE equations are

$$\begin{aligned} dx &= \sqrt{2\kappa dt} W \\ dz &= v dt, \end{aligned} \quad (4)$$

where W is a Wiener process, described as a Gaussian random number with unity variance and zero mean.¹ The solution given by Equations (4) is equivalent to Equation (3). We can easily see that after a time t the pseudoparticles solved with Equation (4) are at $z = vt$, and spread along the x with variance $\langle x^2 \rangle = 2\kappa t$. However, physically the particle propagating with velocity v can only have propagated a maximum distance of $s = vt$ in time t . Thus, the distance the particles have propagated along the x -axis is not taken physically into account in Equation (2).

¹ Note that the Wiener process is often formally written as having $\langle W(t)^2 \rangle = t$, or $\langle dW^2 \rangle = dt$. However, in applications it is often more convenient to consider the dependence of the process on time separately.

To develop a discussion on how the unphysicality of the diffusion equation can be taken into account we define the pathlength s of a particle integral of

$$ds = v dt, \quad (5)$$

that is, the pathlength of the particle is defined as the distance a particle propagates with velocity v in time dt . As can be seen in Equation (4), for the *diffusion solution* the pathlength of the particle is given as

$$s_{\text{diff}} = \int_P dz. \quad (6)$$

What this means is that as the particle propagates along a stochastic path P , the distance the particle diffuses across the field, dx , does not “consume time,” and thus according to the definition of Equation (5), does not contribute to the pathlength. The practical consequence of this is that if we consider the arrival time of a particle from, say, the origin to a point (X, Z) , the solution of Equation (2) gives $t = vZ$, thus a too-early arrival time compared even to a nondiffusing particle propagating along the direct path, for which $t = v\sqrt{X^2 + Z^2}$.

2.2. Pathlength and Stochastic Differential Equations

As discussed above, the solution of the diffusion-convection equation, Equation (2), gives too-early onsets, or too short pathlengths, for particles with a finite velocity. However, the SDE approach to solving the diffusion-convection equation provides an opportunity to estimate the distance propagated by the particle as an SDE steplength

$$\delta s_{\text{SDE}} = \sqrt{\delta x^2 + \delta z^2}, \quad (7)$$

that is, calculating the length of each stochastic 2D step that can then be used to evaluate the time required for taking the step, $\delta t = \delta s/v$.

Let us investigate this approach further. Using Equation (4) we obtain

$$\delta s_{\text{SDE}} = v \delta t \left(\frac{2\kappa W^2}{v^2 \delta t} + 1 \right)^{1/2}. \quad (8)$$

We can define $T_z \equiv N\delta z/v \equiv Z/v$, where Z is the distance propagated along the z -direction in time T_z , and $T_z = N\delta t$ is the corresponding time, excluding any contribution from stepping in the x -direction. Using these, we have

$$\delta s_{\text{SDE}} = v \frac{T_z}{N} \left(\frac{2\kappa W^2}{v^2 T_z} N + 1 \right)^{1/2}. \quad (9)$$

We can now evaluate the pathlength of the particle due to N SDE steps, estimating W^2 as unity,² to be

$$s_{\text{SDE}} \sim v T_z \left(\frac{2\kappa}{v^2 T_z} N + 1 \right)^{1/2}. \quad (10)$$

² Note that Equation (8) could be further developed using Itô calculus (e.g., Gardiner 2009). However, it is easy to see that the integral diverges at the limit of $\delta t \rightarrow 0$, rendering use of Itô calculus not useful.

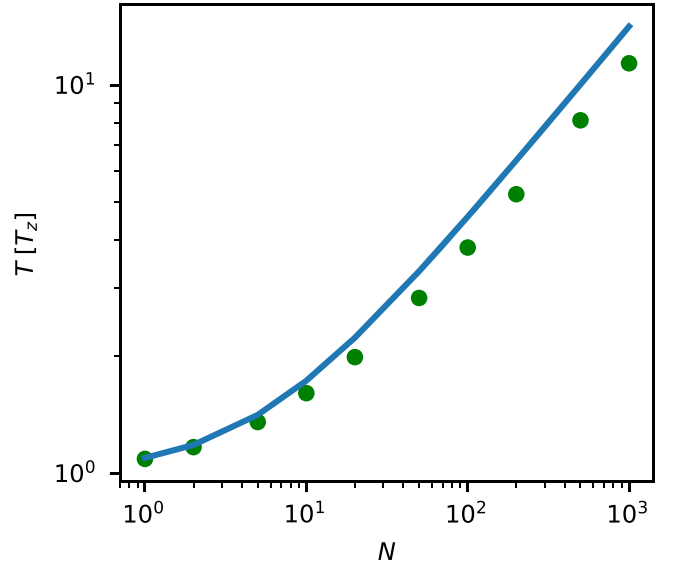


Figure 1. Dependence of propagation time T_{SDE} on the number of steps N , for $\kappa = 0.1$ for total time $T_z \equiv N\delta t = 1$. The curve shows the length given by Equation (11), and the symbols show the results of SDE simulations, where at each step the distance propagated is calculated from Equation (7).

Thus, the time required for the particle to propagate the path would be

$$T_{\text{SDE}} = \frac{s_{\text{SDE}}}{v} \sim T_z \left(\frac{2\kappa}{v^2 \delta t} + 1 \right)^{1/2}. \quad (11)$$

As can be clearly seen in Equations (10) and (11), the approach for estimating the pathlength using Equation (7) results in an unphysical solution, as the obtained distance s_{SDE} , and consequently the propagation time T_{SDE} , depends on the selected timestep length, δt . For large timesteps, the total propagation time given by Equation (11) approaches T_z , that is, it has no contribution from the diffusive steps taken across the z direction. At small timesteps, the propagation timescales as $\delta t^{-1/2}$, or $N^{1/2}$, approaching infinity. The propagation time scaling as $N^{1/2}$ is consistent with the fractal dimension $D = 2$ of the path of a particle in Brownian motion (e.g., Mandelbrot 1982; Rapaport 1985).

We demonstrate the dependence of the pathlength of a random-walking particle on the steplength further by simulating pseudoparticles using the SDE Equations (4) and calculating the pathlength with Equation (7). In Figure 1, we show the resulting $T = s/v$ for parameter values $\kappa = 0.1$, $v = 1$, and $T_z = 1$, with the filled circles showing the mean T for 10,000 pseudoparticles as a function of the number of timesteps, N . The solid curve shows the analytical expression given by Equation (11). The simulations show clearly both the asymptotic $N^{1/2}$ at large N , and the approach to unity at small N , as predicted by Equation (11).

Thus, it appears that the method of using Equation (7) for evaluating the pathlength of the particles provides an unphysical result: the pathlength depends on how we select the timestep lengths. In general, we are not free to determine this timestep arbitrarily. It is typically determined so that the number of timesteps is large, to ensure $N \gg 1$ and to obtain sufficiently large statistical distribution of the steps. The timestep is also limited by the possible spatial and temporal variation of the diffusion coefficient (and other terms such as the background magnetic field in heliospheric magnetic field

configuration): such properties should not change appreciably during the SDE step.

It is easy to see that the problems arising from using Equation (7) for pathlength determination are not limited to our simple diffusion-convection Equation (2): similar results can be derived also for two- or three-dimensional problems where propagation in one or more directions is diffusive. For spatial diffusion in two Cartesian directions x and z , the pathlength would be

$$s_{\text{SDE},2\text{D}} \sim T_d \left(\frac{2\kappa_x + 2\kappa_z}{\delta t} \right)^{1/2}, \quad (12)$$

where $T_d = N\delta t$. Thus, the pathlength depends on δt also for two- and three-dimensional spatial diffusion in the SDE picture. This is a direct consequence of the pathlength of a random-walking particle being fractal, which results in infinite pathlength for an infinitesimal stepsize (e.g., Mandelbrot 1982).

However, as noted by Rapaport (1985), in real physical situations the pathlength of a random-walking particle is not infinite, but limited by the physics behind the random-walking process. Thus, in order to evaluate the pathlength of particle propagating in stochastic magnetic fields, we must understand the physics behind the random walk.

2.3. Pathlength and Gaussian Random Walk of Magnetic Fieldlines: Turbulent Islands and Ultrascale

The evaluation of the pathlength from the SDE steps in x and z directions, as given by Equation (7), proved unphysical. However, it does provide a possibility to solve the problem of determining the pathlength of a diffusing particle, given a suitable physical framework. Here, we employ field-line random walk as the framework for determining the pathlength of a diffusing particle.

In the SDE method, the stepsize does not have a physical meaning, but in the physical world it does. Particle cross-field diffusion is believed to be dominated by their following the turbulent random-walk of the magnetic fieldlines (e.g., Fraschetti & Jokipii 2011). The fieldlines do not, however, meander at infinitesimal scales, since physical processes damp small-scale fluctuations. Thus, a length scale that would describe the meandering of the fieldlines is a good candidate for evaluation of the pathlength of a particle in turbulent magnetic fields.

Such a length scale can be derived from the definition of a fieldline diffusion coefficient and the concept of an ultrascale, $\tilde{\lambda}$. The fieldline diffusion coefficient for 2D-dominated turbulence is given by

$$D_{\text{FL}} = \frac{\tilde{\lambda} \sqrt{\delta B_{\perp}^2/2}}{B}, \quad (13)$$

where B is the magnitude of the ambient background magnetic field, and δB_{\perp}^2 is the turbulence variance (Matthaeus et al. 1995). For 2D turbulence spectrum $S(k)$, the ultrascale is defined as

$$\tilde{\lambda}^2 = \frac{\int S(k) k^{-2} dk}{\delta B^2}, \quad (14)$$

where k is the wavenumber.

Matthaeus et al. (1999) gives the ultrascale an interpretation as the representative scale size of turbulent closed magnetic 2D

structures, “magnetic islands,” in the cross-field direction, x . The fieldlines in 2D-dominated turbulence can be thought to be either trapped in magnetic islands or meandering freely around these islands (Ruffolo et al. 2003; Chuychai et al. 2007). We can thus consider the ultrascale to be the relevant cross-field length scale for the meandering of the untrapped fieldlines around the islands that are of size $\tilde{\lambda}$.

The distance Δz_{FL} along the mean field direction as the fieldline propagates a cross-field length $\tilde{\lambda}$ can then be evaluated using the fieldline diffusion coefficient, Equation (13), using the general definition of a diffusion coefficient $D_{\text{FL}} = \langle \Delta x_{\text{FL}}^2 \rangle / (2\Delta z_{\text{FL}})$, where the distance along the z -axis takes the place of time in the denominator for fieldline diffusion. If we consider the mean square cross-field step given as the ultrascale, $\langle \Delta x_{\text{FL}}^2 \rangle = \tilde{\lambda}^2$, we can write

$$\Delta z = \frac{\tilde{\lambda}^2}{2D_{\text{FL}}} = \tilde{\lambda} \frac{B}{\sqrt{2\delta B^2}}. \quad (15)$$

Equation (15) gives a natural interpretation to the fieldline diffusion coefficient in Equation (13): the fieldline random walk across the mean field direction is described as random walk with stepsize $\tilde{\lambda}$, with the ratio between the steps along and across the field, $\Delta z_{\text{FL}}/\Delta x_{\text{FL}}$, equal to $B/\delta B_{\perp}$.

Using the steplength as defined by the turbulent island size, given by Equation (15), we can solve the pathlength of the meandering fieldline as *Gaussian random walk* with

$$\Delta x_{\text{FL}} = \sqrt{2D_{\text{FL}}\Delta z_{\text{FL}}} W. \quad (16)$$

The pathlength of a particle following such a fieldline can then be estimated and integrated using equation

$$s_{\text{FL}} = \sum_i \sqrt{\Delta z_{\text{FL},i}^2 + \Delta x_{\text{FL},i}^2}, \quad (17)$$

with the steps along and across the field given by Equations (15) and (16), respectively. Analogously, the pathlength of a particle following a fieldline meandering around turbulent magnetic islands without scattering has a pathlength

$$s = \sum_i \sqrt{\Delta z_i^2 + \Delta x_i^2}, \quad (18)$$

where $\Delta z_i = \Delta z_{\text{FL},i}$ and $\Delta x_i = \Delta x_{\text{FL},i}$. In the following, we will drop the subscript FL for convenience, with the symbols prepended with Δ referring to paths due to meandering around magnetic islands.

2.4. Statistical Evaluation of the Length of a Meandering Path

To estimate the length of a meandering fieldline, it is useful to derive an expression that uses statistical properties of the turbulence giving rise to the meandering of fieldlines. Furthermore, we are usually interested in the pathlength of the particles to a given location in space, such as Earth, relative to the particle source. Here we will derive an expression for pathlength as a function of the observer coordinates relative to the particle source and turbulence properties, for our Cartesian geometry case with constant background magnetic field.

Consider a path of a particle from the origin (0, 0) to some point (X, Z), due to the Gaussian random walk process. The step across the mean field is given by Equation (16). The mean pathlength $\langle s \rangle$ would then be the mean length given by

Equation (18) of all possible paths between the origin and (X, Z) .

To evaluate the pathlength, we decompose the cross-field step to a systematic part, $\Delta x_{a,i}$ which will move the particle the cross-field distance $X = \sum_i \Delta x_{a,i}$, and a stochastic part $\Delta x_{s,i} = \sqrt{2D_{\text{FL}}\Delta z_i} W_i$ with $\langle \Delta x_{s,i} \rangle = 0$, and $\langle \Delta x_{s,i}^2 \rangle = 2D_{\text{FL}}\Delta z_i$. With these definitions, the steplength is given as

$$\Delta s_i = \sqrt{\Delta z_i^2 + (\Delta x_{a,i} + \sigma_i W_i)^2}, \quad (19)$$

where $\sigma_i = 2D_{\text{FL}}\Delta z_i$. We can further define the length of the systematic step, $(\Delta x_{a,i}, \Delta z_i)$, as

$$\Delta s_{0,i} = \sqrt{\Delta z_i^2 + \Delta x_{a,i}^2},$$

noting that $s_0 \equiv \sum s_{0,i} = \sqrt{X^2 + Z^2}$ is the distance between $(0, 0)$ and (X, Z) along a straight line.

Using the notations given above, we expand Equation (19) to second order in $\sigma_i W_i$ to give

$$\Delta s_i \approx \Delta s_{0,i} + \frac{\sigma_i \Delta x_{a,i}}{\Delta s_{0,i}} W_i + \frac{\sigma^2 \Delta z_i^2}{2\Delta s_{0,i}^3} W_i^2. \quad (20)$$

Averaging this over the Wiener process W , and noting that $\langle W \rangle = 0$ and $\langle W^2 \rangle = 1$, we find the mean length of the step

$$\langle \Delta s_i \rangle \approx \Delta s_{0,i} \left(1 + \frac{D_{\text{FL}} \Delta z_i^3}{\Delta s_{0,i}^4} \right). \quad (21)$$

Substituting from Equations (13) and (15), we get a simpler form,

$$\langle \Delta s_i \rangle \approx \Delta s_{0,i} \left(1 + \frac{\delta B^2 Z^4}{B^2 s_0^4} \right). \quad (22)$$

If we further assume that $\delta B^2/B^2$ is constant, we find for the mean pathlength

$$\langle s \rangle \approx s_0 \left(1 + \frac{\delta B^2 Z^4}{B^2 s_0^4} \right). \quad (23)$$

Note that the term $Z/s_0 = \cos \alpha$, where α is the angle between the z -axis and the line connecting the origin and the point (X, Z) . Thus, the term $(Z/s_0)^4$ is 1 for $X = 0$ and decreases to 0 for larger values of $|X|$.

This form is beneficial in that it depends only on the statistical properties of the turbulence, and it does not depend on the variables describing the steplength. It should be noted that this analysis is valid only for $\sigma < \Delta s_0$, that is, $D_{\text{FL}} < \Delta z$ which, according to our definitions in Equations (13) and (15) holds for $\delta B^2 < B^2$, a valid assumption in the inner heliosphere.

In Figure 2, we plot the mean pathlength as given by Equation (23) together pathlengths derived from SDE simulations of magnetic fieldline meandering, with the pathlength calculated using Equation (18). In the simulations, paths are started from the origin, and propagated until they reach distance $Z = 1$ au along the fieldline, with the pathlength calculated as the sum of lengths given by Equation (19). In Figure 2 the contours represent the probability density of simulated pathlengths as a function of the final position $(X, Z = 1)$, for simulation parameters $N = 10$ and $D_{\text{FL}} = 0.03$ au, corresponding to the values in Laitinen et al. (2016) at 1 au,

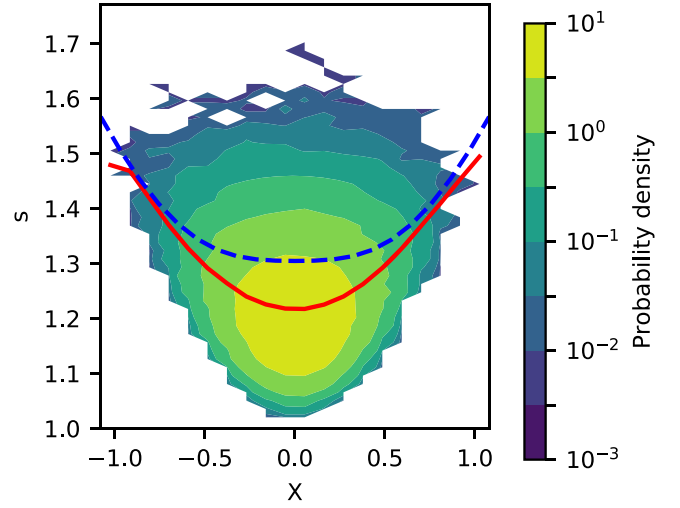


Figure 2. Dependence of pathlength s on the total cross-field deviation X after $N = 10$ Gaussian random walk steps, with $D_{\text{FL}} = 0.03$ au and the integrated distance along the mean field direction, $Z = 1$ au. The contours show the probability density of the path lengths obtained from Gaussian random walk simulations, and the solid red curve the mean pathlength of the simulated particles as a function of X . The blue dashed curve shows the result of Equation (23).

resulting in $\sigma = 0.078$ au. The dashed blue curve shows Equation (23), whereas the solid red curve shows the mean pathlength obtained from the simulations, as a function of X . As we can see, the mean pathlength is well-reproduced by the estimate, thus similar estimates could be used to analyze the pathlength also in more complicated scenarios. The shortest distances in Figure 2 follow the length of a direct path between the origin and (X, Z) , $s_0 = \sqrt{X^2 + Z^2}$. The shortest pathlength for statistics of 100,000 paths is 1.013 au.

3. Pathlength in Parker Spiral Configuration

We will now consider the length of the meandering path in the context of a Parker spiral field. We limit this study to 2D, in the heliographic equatorial plane; however, the same method can easily be extended to 3D. In 2D, the Parker spiral can be represented as a polar Archimedean curve

$$r = \phi_0 + a\phi, \quad (24)$$

where r is the heliocentric distance, ϕ heliolongitude, and $a = V_{\text{sw}}/(\Omega_0 \sin \theta)$, with $\Omega_0 = -2.86533 \times 10^{-6}$ rad s^{-1} the solar rotation rate, $\theta = 90^\circ$ the colatitude at the heliographic equator, and V_{sw} the solar wind speed. We use $a = -1$, which corresponds to $V_{\text{sw}} = 430$ km s^{-1} .

Within the simulations presented below, the paths are traced in a locally Cartesian frame with one axis along the Parker spiral, with stochastic steps across the Parker spiral direction. This is the method adopted in several studies SEP transport is analyzed by solving a 3D particle transport equation with SDE equations (e.g., Zhang et al. 2009; Dröge et al. 2010).

We use a fieldline diffusion coefficient D_{FL} similar to that in Laitinen et al. (2016). However, in this paper we use an analytic formulation based on the ultrascale λ (Matthaeus et al. 2007), given in the Appendix, instead of integrating the turbulence spectrum as in Laitinen et al. (2016). Both approaches are consistent with Matthaeus et al. (1995).

As in Section 2, we will consider three methods for calculating the pathlength.

3.1. Pathlength and Diffusion Solution

The SDE for a diffusively random-walking fieldline is given as³

$$dr_{l,\phi} = \sqrt{2dlD_{\text{FL}}(r)} W, \quad (25)$$

where dl is a step along the local Parker spiral direction, and $dr_{l,\phi}$ a step normal to the Parker spiral in the equatorial plane. As discussed in Section 2.1, the cross-field steps do not contribute to the propagation time under the diffusion description. Thus, for the diffusion solution case in Parker spiral configuration, the pathlength is given as

$$s_{\text{diff}} = \int_P dl, \quad (26)$$

where P is the path determined by Equation (25).

Within the numerical solution of Equation (25) the SDE step along the Parker spiral, dl , is limited by the variation of the diffusion coefficient D_{FL} , as well as the changing geometry of the system as the path meanders across the Parker spiral geometry: none of $D_{\text{FL}}(r)$, the Parker spiral direction, nor the direction across the local Parker spiral can be allowed to change appreciably during the step given by Equation (25). We have chosen to use the scale length of the magnetic field, $L_B = B/(\partial B/\partial r) \sim 2r$, as a representative scale of change of the inner heliosphere, and use $\Delta l = 0.01 r$ so that the changes in the background medium would be small within the SDE step.

To solve the fieldline path, we use a leapfrog scheme, where the magnitude and direction of the $dr_{l,\phi}$ step is evaluated at the midpoint between two consecutive steps along the Parker spiral.

3.2. Pathlength and Stochastic Differential Equations

Solution of the SDE steplength, as defined in Section 2.2, is given for Parker spiral by Equations

$$\delta r_{l,\phi} = \sqrt{2\delta l D_{\text{FL}}(r)} W. \quad (27)$$

$$s_{\text{SDE}} = \sum_i \sqrt{\delta l_i^2 + \delta r_{l,\phi,i}^2}. \quad (28)$$

The SDE given by Equation (27) is equivalent to the diffusion case, Equation (25), only the determination of the pathlengths differ. The integration scheme is the same as in the first case. Likewise, we use the same steplength as in the first case, $\delta l_i = 0.01 r$.

3.3. Pathlength and Gaussian Random Walk of Fieldlines

Solution of the Gaussian random walk steplength in Parker geometry is given by

$$\Delta l = \frac{\tilde{\lambda}^2}{2D_{\text{FL}}}, \quad (29)$$

$$\Delta r_{l,\phi} = \sqrt{2\Delta l D_{\text{FL}}(r)} W, \quad (30)$$

³ It should be noted that depending on the physics of the underlying processes, a term proportional to the gradient of D_{FL} (or divergence of the diffusion tensor) is typically included in Equation (25). However, we neglect it as a small term compared to dl and $dr_{l,\phi}$.

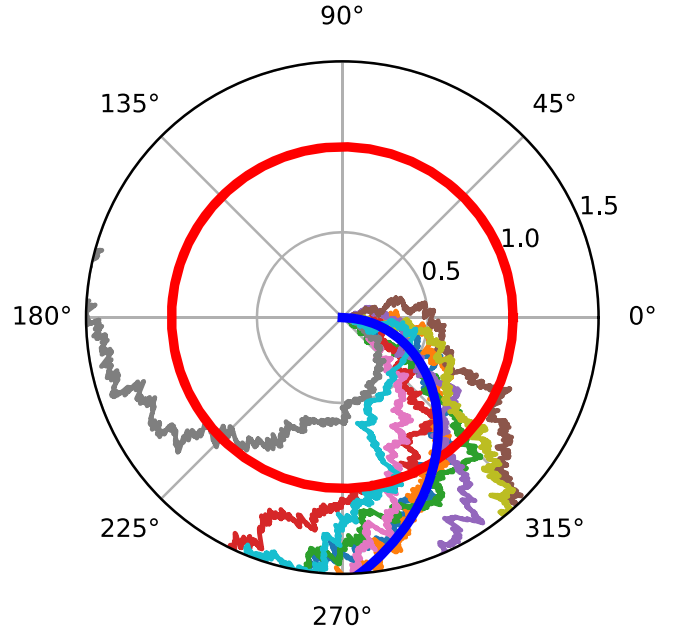


Figure 3. Sample of stochastically meandering fieldlines, simulated with steplength $dl = 0.01 r$ au along the Parker spiral, and field-line diffusion coefficient given by Equation (36). The thick red curve is at 1 au radial distance from the Sun, and the thick blue curve shows the Parker spiral for solar wind velocity $V_{\text{sw}} = 430 \text{ km s}^{-1}$.

$$s_{\text{GRW}} = \sum_i \sqrt{\Delta l_i^2 + \Delta r_{l,\phi}^2}. \quad (31)$$

For the ultralength, we use $\tilde{\lambda} = \sqrt{\lambda_c L}$ (see the Appendix), with $\lambda_c = 0.007 \text{ au}$ and $L = r$, as in Laitinen et al. (2016). As both $\tilde{\lambda}^2$ and D_{FL} are proportional to r for most of the space inside 1 au in our model, the Equation (15) results in a roughly constant meandering length scale $\Delta l = 0.1 \text{ au}$. We note that our value of λ_c results in ultrascale $\tilde{\lambda} = 0.08 \text{ au}$ at 1 au, consistent with the simulation results in Ruffolo et al. (2003), who discussed their simulations with $\tilde{\lambda} = 0.06 \text{ au}$ in the context of SEP intensity dropouts over scales $\sim 0.03 \text{ au}$. Flux ropes of similar scales have also been observed in situ in the heliosphere, with Yu et al. (2016) finding a median size of 0.02 au for small-scale flux ropes at STEREO spacecraft.

As the step $\Delta l = 0.1 \text{ au}$ is quite long and may cause numeric errors, we integrate the pathlength as in the previous two cases, but then interpolate the (r, ϕ) coordinates at distances $\Delta l = 0.1 \text{ au}$. Other methods, such as smoothing the path with an appropriate kernel of length determined by Equation (15) before integrating the length can also be used.

4. Results

We use the model presented in Section 3 to study the length of meandering fieldlines in the heliosphere. The paths are started from a point at the solar surface, at $(r = r_\odot, \phi = 0)$.

In Figure 3, we show a sample of meandering paths in the inner heliosphere, obtained from our model. The thick blue curve depicts the Parker spiral starting from longitude $\phi = 0$, which crosses the 1 au distance (red circle) at longitude $\phi = -1 \text{ rad}$, or 303° . It should be noted that the meandering paths can cross the 1 au sphere several times, and from both inside and outside of Earth's orbit, due to the curving of the Parker spiral.

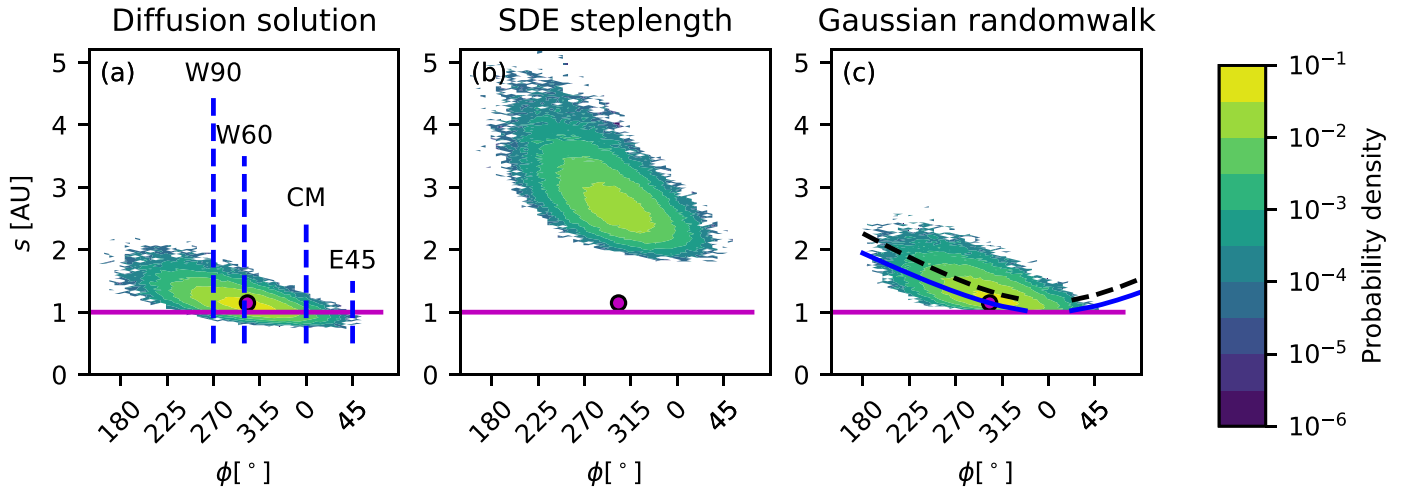


Figure 4. Probability density of pathlengths s as a function of heliointitude, ϕ , at a heliocentric distance of 1 au. The pathlengths are integrated (a) as the sum of the steplengths along the Parker spiral Equation (26); (b) sum of SDE steplengths using Equation (28) with $\delta l = 0.01r$; and (c) with Gaussian random walk using Equation (31), with the steplength given by Equation (29). The horizontal line shows pathlength of 1 au, and the magenta-filled circle is at $\phi = 303^\circ$, the longitude connected to the source longitude $\phi = 0^\circ$ at the Sun, and $s = 1.15$ au, the nominal Parker spiral length. The blue vertical dashed lines in panel (a) correspond to Solar source longitudes as viewed by an observer at Earth. The solid blue curve and dashed black curve in panel (c) show the estimated mean pathlength using Equation (33) for $\rho = 0$ and $\rho = 1$, respectively.

To analyze the pathlengths, we follow the fieldlines to a total distance along the Parker spiral of $l = 5.6$ au. Each time the path crosses radial distance of 1 au from the Sun, we record the heliointitude of the crossing and the length the meandering path as defined in Equations (26), (28), and (31), for the three methods.

In Figure 4, we show the probability density of the integrated pathlength of the meandering paths at 1 au radial distance, as a function of heliointitude. The horizontal line shows pathlength of 1 au, whereas the magenta-filled circle is at the longitude and pathlength for the nominal Parker spiral connected to $\phi_0 = 0^\circ$ at the Sun along the nominal Parker spiral for $a = -1$, that is $\phi = 303^\circ$ and $l = 1.15$ au. The labeled blue vertical dashed lines describe the solar longitude of the source as would be seen by an observer at Earth. The label CM, at $\phi = 0^\circ$, corresponds to a source at the center of solar disk, center meridian, whereas W60 depicts a well-connected western source and E45 a poorly connected eastern source. The label W90 represents the western limb, thus longitudes on its left side represent connection to backside events.

In panel (a), we show the pathlength calculated as given by the diffusion solution, as given by Equation (25), that is, just taking into account the distance propagated along the Parker spiral, corresponding to the SDE solution of spatial cross-field diffusion of fieldlines, as discussed in Section 2.1. As can be clearly seen, the shortest pathlengths are shorter than the distance from the Sun to 1 au (horizontal line). This corresponds to the unphysically early SEP onset times in SEP transport simulations with spatial diffusion, which was discussed in Strauss & Fichtner (2015).

In panel (b) of Figure 4, we show the pathlength of a meandering fieldline in the Parker spiral geometry as calculated with SDE steplengths, with Equation (28). While these pathlengths are not unphysically short as in panel (a), they are very long, contradicting observations analyzed with the VDA method (e.g., Paassilta et al. 2017, and other references cited in Section 1). As discussed in Section 2.2, this is an artificial feature due to the fractal nature of the pathlength of

random walk, which results in unphysical dependence of the pathlength on the adopted stepsize, $\delta l = 0.01r$.

We now turn to using the concept of Gaussian random walk of magnetic fieldlines discussed in Section 2.3, where we derived a physically meaningful scale length for the meandering of fieldlines. We show the probability density of the pathlengths in Figure 4(c), as calculated with Equation (31). As can be seen, for the Gaussian random walk case the pathlengths range between 1 and 3 au at all heliointitudes, with well-connected ($\phi = 303^\circ$, magenta-filled circle) longitudes having pathlengths ranging from 1 to 2 au, with the most probable pathlength being slightly longer than the nominal 1.15 au for the 430 km s^{-1} solar wind. For events occurring on most parts of the solar disk our result suggests that the pathlength can be shorter than the nominal Parker spiral length, down to 1 au. The short pathlengths are caused by the stochastic paths that are “straightened” from the Parker spiral shape to radial shape. It should be noted though, that the probability of such paths is low. Also notable is the vanishingly small probability of paths that reach heliointitudes larger than $\phi \sim 45^\circ$. This is consistent with the rarity of SEP events originating from solar eruptions farther in the eastern heliointitudes, east from E45.

For SEP events on the western hemisphere (between the vertical dashed lines labeled CM and W90 in Figure 4), the shortest pathlengths are still of the order of or shorter the nominal Parker spiral length, 1.15 au, and only sources far behind the western limb (left of the vertical dashed line labeled W90) have substantially longer shortest pathlengths. Thus, the onsets of even some backside events could result in close to nominal pathlengths. The mean pathlength, however, increases significantly for western hemisphere and behind-the-limb sources.

As discussed in Section 2.4, the mean length of a meandering path can be estimated using the statistical values of the meandering path. For Parker geometry, such estimation is not as simple as in the Cartesian case, as the “direct path” with length s_0 in Equation (23), or the statistical distribution of steps within the meandering path, cannot be determined unambiguously. We approach the estimation by evaluating

the direct path with a Parker spiral that joins the source longitude $\phi_0 = 0^\circ$ to a longitude ϕ_r at a given distance r . Such an undisturbed Parker spiral, parameterized with $a = r/\phi_r$, has length of

$$s_0(r, \phi_r) = \frac{r}{2\phi_r} [\phi_r \sqrt{1 + \phi_r^2} + \ln(\phi_r + \sqrt{1 + \phi_r^2})]. \quad (32)$$

As we saw in Section 2.4, in the case of Cartesian geometry an undisturbed path experienced lengthening by a factor of $(1 + \rho \delta B^2/B^2)$ due to stochastic wandering (Equation (23) with $\rho = Z^4/s^4 \in [0, 1]$). Applying similar statistical lengthening to the undisturbed Parker spiral length, given by Equation (32), thus we can write the mean length of a stochastic path from a point source at the Sun at $\phi = 0$ to (r, ϕ_r) as

$$\langle s(r, \phi_r) \rangle = s_0(r, \phi_r) \left[1 + \rho \frac{dB^2}{B^2} \right]. \quad (33)$$

Evaluating $\langle dB^2/B^2 \rangle = 0.16$ between 1/215 au and 1 au for our turbulence model,⁴ we show Equation (33) in Figure 4(c) with a solid blue curve for $\rho = 0$ and a dashed black curve for $\rho = 1$. As can be seen, the black curve traces well the most likely pathlengths for western sources (left from W60, magenta symbol), whereas the eastern pathlengths tend to be shorter, closer to the $\rho = 0$ curve.

5. Discussion

In this study, we have investigated the pathlength of SEPs propagating along interplanetary magnetic fieldlines that spread stochastically across the mean magnetic field due to fieldline random walk. As we demonstrate in Section 2, the diffusion description of such motion neglects the effect of the stochastic cross-field motion in evaluation of distance the particle can propagate in a given time, resulting in erroneous first-arrival time of SEPs to a given distance. We introduced ultrascale, the scale size of the turbulent islands (Matthaeus et al. 1999), as the physically justified characteristic scale of the fieldline meandering, and used this concept to evaluate the pathlength of the meandering fieldline. The resulting pathlengths are realistic, and do not exhibit the break of causality discussed in Strauss & Fichtner (2015).

It is important to note that the length of the path traveled by the SEPs is not the only problem encountered when applying timing analysis methods such as the VDA for SEPs. The evolution of SEP intensities in the interplanetary space is a combined effect of the length of the meandering paths, scattering of the particles along the path (Lintunen & Vainio 2004; Sáiz et al. 2005), and propagation across the meandering fieldlines due to diffusive escape from one path to another (Laitinen & Dalla 2017) and drifting due to the large-scale curvature and gradients of the background Parker spiral magnetic field (Dalla et al. 2013). This is compounded with the pre-event background intensities (Laitinen et al. 2015), which make it difficult to determine when the “first nonscattered” particles would have arrived.

Thus, while the shortest pathlengths in Figure 4(c) at W60 are around 1 au, it may be that the number of particles

propagating at the low-probability short paths are not seen above the pre-event background. Similarly, while the mean pathlength at $\sim 225^\circ$ (W135, behind the western limb) is around 2 au, the first observed particles may have traversed the shorter paths with similar or only slightly lower probability. At large heliolongitudinal distances from the best-connected site (W60), the first-observed SEPs may have propagated across the fieldlines due to diffusive escape (Laitinen & Dalla 2017) and drifts (Dalla et al. 2013), instead of having propagated directly from the solar source along the meandering fieldlines. All of these factors contribute to uncertainties in SEP timing methods such as the VDA.

For a full understanding of SEP propagation, one should thus combine the analysis of meandering paths and the SEP transport into one framework, to amend the often used diffusion-convection approach used in many SEP and galactic cosmic-ray studies (e.g., Zhang et al. 2009; Dröge et al. 2010; Strauss et al. 2011; Strauss & Fichtner 2015; Wang & Qin 2015). In such a framework, the meandering pathlength should be evaluated using the Gaussian random walk approach introduced in this study, and the propagation time of simulated pseudoparticles should be rescaled by factor $\Delta s/\Delta z$, so that the particle with velocity v would be able to physically take a step $\Delta s = v\Delta t$ in time Δt . This was partly done in Laitinen et al. (2016), where particles propagated along stochastically meandering fieldlines, with additional spatial diffusion from the meandering path, but without the rescaling of the propagation time. In future work, we will incorporate the time-rescaling to the Laitinen et al. (2016) model.

6. Conclusions

In this paper, we have discussed the problem of calculating the time that diffusively propagating particles take to travel from their source to the observer, noting that such evaluation cannot be provided by the standard spatial diffusion approach. We have shown that pathlengths derived using the SDE steplength are very sensitive to the selected stepsize, and thus not physical. We introduced the concept of Gaussian random walk of magnetic fieldlines with physically justified steplengths as derived from the turbulence ultrascale to provide an estimate for the distribution of pathlengths. This approach, when applied to a Parker spiral configuration, produces pathlengths that are consistent with observations. We find that at 1 au for Parker spiral with solar wind velocity of 430 km s^{-1} , the shortest pathlengths are close to the nominal Parker spiral length, or even shorter, for a large range of heliolongitudes, corresponding to SEP events taking place at E45 to W90 solar longitudes when viewed from Earth. The mean pathlength increases roughly linearly from the nominal 1.15 au for SEP events originating at W60 to far beyond the western limb. Our method should be used to correct for propagation time in all spatial diffusion SDE codes, when the physical scales for the underlying random walk process can be estimated.

T.L. and S.D. acknowledge support from the UK Science and Technology Facilities Council (STFC; grant ST/R000425/1), and the International Space Science Institute as part of international team 297. Access to the University of Central Lancashire’s High Performance Computing Facility is gratefully acknowledged.

⁴ Note that this value differs from Laitinen et al. (2016) where the diffusion coefficient was calculated via integrating the spectrum, whereas here we use the unnormalized $\tilde{\lambda} \sim \sqrt{\lambda_c L}$ from Matthaeus et al. (2007), see the Appendix.

Appendix

Analytic Expression for Fieldline Diffusion Coefficient

Laitinen et al. (2016) used a spectrum with a flat spectrum at scales between the largest scale in the spectrum, L , and the bendover scale λ_c , and Kolmogorov spectrum at scales smaller than λ_c . As discussed in Matthaeus et al. (2007), for such a spectrum the ultrascale is given as $\tilde{\lambda} \sim \sqrt{\lambda_c L}$. Laitinen et al. (2016) took $L \propto r$, the radial distance from the Sun, a natural choice in a spherically expanding, outflowing turbulent plasma.

For the turbulence amplitude Laitinen et al. (2016) used the WKB approximation,

$$\delta B^2(r) = \delta B^2(r_0) \left(\frac{r_0}{r} \right)^3 \left(\frac{V_{sw,0} + v_{A0}}{V_{sw,0} + \frac{r_0}{r} v_{A0}} \right)^2, \quad (34)$$

where V_{sw} and v_A are the solar wind velocity and Alfvén velocity, and values subscripted with 0 are those at reference distance $r = r_0$. The Parker spiral magnetic field magnitude is given by

$$B(r) = B_0 \left(\frac{r_0}{r} \right)^2 \sqrt{\frac{r^2 + a^2}{r_0^2 + a^2}}, \quad (35)$$

where a is the Parker spiral parameter.

Using Equations (13), (34), (35), and $\tilde{\lambda} \propto \sqrt{r}$, we can write for the field-line diffusion coefficient

$$D_{FL}(r) = D_{FL,0} \frac{r}{r_0} \frac{V_{sw,0} + v_{A0}}{V_{sw,0} + \frac{r_0}{r} v_{A0}} \sqrt{\frac{r_0^2 + a^2}{r^2 + a^2}}. \quad (36)$$

We use as reference values at $r_0 = 1$ au, $v_{A0} = 30 \text{ km s}^{-1}$, $V_{sw} = 430 \text{ km s}^{-1}$, and $a = -1$. For the fieldline diffusion coefficient at 1 au, we use $D_{FL,0} = r_0^2 (10^\circ)^2 / \text{au}$, consistent with Laitinen et al. (2016).

ORCID iDs

T. Laitinen  <https://orcid.org/0000-0002-7719-7783>

S. Dalla  <https://orcid.org/0000-0002-7837-5780>

References

- Agueda, N., Lario, D., Vainio, R., et al. 2009, *A&A*, **507**, 981
 Chuychai, P., Ruffolo, D., Matthaeus, W. H., & Meechai, J. 2007, *ApJ*, **659**, 1761
 Cohen, C. M. S., Mason, G. M., Mewaldt, R. A., & Wiedenbeck, M. E. 2014, *ApJ*, **793**, 35
 Dalla, S., Marsh, M. S., Kelly, J., & Laitinen, T. 2013, *JGRA*, **118**, 5979
 Dalla, S., Balogh, A., Krucker, S., et al. 2003, *AnGeo*, **21**, 1367
 Dresing, N., Gómez-Herrero, R., Klassen, A., et al. 2012, *SoPh*, **281**, 281
 Dröge, W. 2003, *ApJ*, **589**, 1027
 Dröge, W., Kartavykh, Y. Y., Dresing, N., Heber, B., & Klassen, A. 2014, *JGRA*, **119**, 6074
 Dröge, W., Kartavykh, Y. Y., Klecker, B., & Kovaltsov, G. A. 2010, *ApJ*, **709**, 912
 Fraschetti, F., & Jokipii, J. R. 2011, *ApJ*, **734**, 83
 Gardiner, C. W. 2009, *Stochastic Methods*, Vol. 13 (4th ed.; Berlin: Springer)
 Gómez-Herrero, R., et al. 2015, *ApJ*, **799**, 55
 He, H.-Q., Qin, G., & Zhang, M. 2011, *ApJ*, **734**, 74
 Jokipii, J. R. 1966, *ApJ*, **146**, 480
 Jokipii, J. R., & Parker, E. N. 1968, *PhRvL*, **21**, 44
 Kallenrode, M., & Wibberenz, G. 1990, *Proc. ICRC*, **5**, 229
 Kallenrode, M. B. 1993, *JGR*, **98**, 19037
 Krucker, S., & Lin, R. P. 2000, *ApJL*, **542**, L61
 Laitinen, T., & Dalla, S. 2017, *ApJ*, **834**, 127
 Laitinen, T., Dalla, S., & Marsh, M. S. 2013, *ApJL*, **773**, L29
 Laitinen, T., Huttunen-Heikinmaa, K., Valtanen, E., & Dalla, S. 2015, *ApJ*, **806**, 114
 Laitinen, T., Kopp, A., Effenberger, F., Dalla, S., & Marsh, M. S. 2016, *A&A*, **519**, A18
 Laitinen, T., Klein, K.-L., Kocharov, L., et al. 2000, *A&A*, **360**, 729
 Lin, R. P., Potter, D. W., Gurnett, D. A., & Scarf, F. L. 1981, *ApJ*, **251**, 364
 Lintunen, J., & Vainio, R. 2004, *A&A*, **420**, 343
 Mandelbrot, B. B. 1982, *The Fractal Geometry of Nature* (New York: Freeman)
 Matthaeus, W. H., Bieber, J. W., Ruffolo, D., Chuychai, P., & Minnie, J. 2007, *ApJ*, **667**, 956
 Matthaeus, W. H., Gray, P. C., Pontius, D. H., Jr., & Bieber, J. W. 1995, *PhRvL*, **75**, 2136
 Matthaeus, W. H., Qin, G., Bieber, J. W., & Zank, G. P. 2003, *ApJL*, **590**, L53
 Matthaeus, W. H., Smith, C. W., & Bieber, J. W. 1999, in *AIP Conf. Ser.* 471, *Solar Wind Nine*, ed. S. R. Habbal (Melville, NY: AIP), 511
 Paassilta, M., Papaioannou, A., Dresing, N., et al. 2018, *SoPh*, **293**, 70
 Paassilta, M., Raukunen, O., Vainio, R., et al. 2017, *JWSWC*, **7**, A14
 Parker, E. N. 1958, *ApJ*, **128**, 664
 Parker, E. N. 1965, *P&SS*, **13**, 9
 Rapaport, D. C. 1985, *JSP*, **40**, 751
 Reames, D. V. 2009, *ApJ*, **706**, 844
 Reames, D. V., von Rosenvinge, T. T., & Lin, R. P. 1985, *ApJ*, **292**, 716
 Richardson, I. G., von Rosenvinge, T. T., Cane, H. V., et al. 2014, *SoPh*, **289**, 3059
 Ruffolo, D., Matthaeus, W. H., & Chuychai, P. 2003, *ApJL*, **597**, L169
 Ruffolo, D., Pianpanit, T., Matthaeus, W. H., & Chuychai, P. 2012, *ApJL*, **747**, L34
 Sáiz, A., Evenson, P., Ruffolo, D., & Bieber, J. W. 2005, *ApJ*, **626**, 1131
 Shalchi, A. 2010, *ApJL*, **720**, L127
 Strauss, R. D., & Fichtner, H. 2015, *ApJ*, **801**, 29
 Strauss, R. D., Potgieter, M. S., Kopp, A., & Büsching, I. 2011, *JGRA*, **116**, A12105
 Strauss, R. D. T., & Effenberger, F. 2017, *SSRv*, **212**, 151
 Torsti, J., Kocharov, L. G., Vainio, R., Anttila, A., & Kovaltsov, G. A. 1996, *SoPh*, **166**, 135
 Torsti, J., Anttila, A., Kocharov, L. G., et al. 1998, *GeoRL*, **25**, 2525
 Tylka, A. J., Cohen, C. M. S., Dietrich, W. F., et al. 2003, *Proc. ICRC*, **6**, 3305
 Vainio, R., Valtanen, E., Heber, B., et al. 2013, *JWSWC*, **3**, A12
 Wang, Y., & Qin, G. 2015, *ApJ*, **799**, 111
 Wiedenbeck, M. E., Mason, G. M., Cohen, C. M. S., et al. 2013, *ApJ*, **762**, 54
 Yu, W., Farrugia, C. J., Galvin, A. B., et al. 2016, *JGRA*, **121**, 5005
 Zhang, M. 1999, *ApJ*, **513**, 409
 Zhang, M., Qin, G., & Rassoul, H. 2009, *ApJ*, **692**, 109
 Zhao, L., Li, G., Zhang, M., et al. 2019, *ApJ*, **878**, 107